ISSN 0021-3640, JETP Letters, 2012, Vol. 96, No. 9, pp. 582–587. © Pleiades Publishing, Inc., 2012.
Original Russian Text © B.B. Straumal, P.V. Protsenko, A.B. Straumal, A.O. Rodin, Yu.O. Kucheev, A.M. Gusak, V.A. Murashov, 2012, published in Pis'ma v Zhurnal Eksperimental'noi i Teoreticheskoi Fiziki, 2012, Vol. 96, No. 9, pp. 651–656.

Contribution of Tilt Boundaries to the Total Energy Spectrum of Grain Boundaries in Polycrystals

B. B. Straumal[a, b, *], P. V. Protsenko[c], A. B. Straumal[b], A. O. Rodin[b], Yu. O. Kucheev[a, b], A. M. Gusak[d], and V. A. Murashov[c]

[a] *Institute of Solid State Physics, Russian Academy of Sciences, ul. Akademika Ossipyana, Chernogolovka, Moscow region, 142432 Russia*
* *e-mail: straumal@issp.ac.ru*
[b] *National University of Science and Technology MISiS, Leninskii pr. 4, Moscow, 119049 Russia*
[c] *Department of Colloidal Chemistry, Faculty of Chemistry, Moscow State University, Moscow, 119899 Russia*
[d] *Department of Theoretical Physics, Faculty of Physics, Cherkassy National University, Cherkassy, 18027 Ukraine*

Received September 25, 2012

By measuring temperatures T_w for the transition from the incomplete to complete wetting of grain boundaries in poly- and bicrystals, the width of the spectrum of tilt grain boundaries and their contribution to the total energy spectrum of grain boundaries in polycrystals have been experimentally estimated. It has been shown that the tilt grain boundaries correspond to a rather narrow (only 5–10%) portion in the total energy spectrum of grain boundaries in polycrystals. In metals with a low stacking fault energy (copper, tin, zinc), the tilt grain boundaries belong to 10–20% of the grain boundaries with the highest transition temperatures T_w (hence, with low energies). In a metal with a high stacking fault energy (aluminum), the values of T_w for the tilt grain boundaries lie nearly in the middle between the minimum ($T_{w,\min}$) and maximum ($T_{w,\max}$) transition temperatures from the incomplete to complete wetting of grain boundaries. This means that grain boundaries with the structure corresponding to a lower energy than that of the symmetric twin boundaries (or stacking faults) can exist in aluminum.

DOI: 10.1134/S0021364012210114

As early as the turn of the 1940s and 1950s, it became clear that the grain boundaries in metals are not at all amorphous spacers between crystallites; on the contrary, they have a definite crystallographic structure. The so-called tilt grain boundaries turned out to be the simplest ones for both theoretical and experimental analysis. They are the boundaries between crystallites, which are rotated with respect to each other about a fixed common crystallographic axis $\langle hkl \rangle$ (usually with low values of the Miller indices) by a certain misorientation angle θ; the rotation axis $\langle hkl \rangle$ lies in the plane of the boundary. It is clear that the $\{hkl\}_1$ planes for one grain coincide (sometimes with a small translation along the rotation axis) with the $\{hkl\}_2$ planes for another grain. Even in the earlier works dealing with individual boundaries, it was shown that the grain boundary energy σ_{GB} gradually grows from zero with θ, attains the maximum value at a certain θ_{max} value, and then again decreases down to zero [1–5]. The value of θ_{max} is determined by the symmetry of the rotation axis $\langle hkl \rangle$. At small angles, the tilt grain boundary consists of an array of lattice dislocations and the $\sigma_{GB}(\theta)$ function is given by the Read–Shockley expression

$$\sigma_{GB} = Gb\theta \ln(\alpha e/2\pi\theta)/[4\pi(1-\nu)], \qquad (1)$$

where b is the Burgers vector of lattice dislocations, G is the shear modulus, ν is the Poisson ratio, and α is a numerical constant, which is about unity for crystals with the face-centered cubic (fcc) lattice and ranges from one to four in crystals with the body-centered cubic (bcc) lattice [7].

Later, it was found that, at certain values of the misorientation angle θ_Σ, there arise so-called coincidence site lattices (CSLs). They are superlattices common to two lattices of the rotated grains (grains 1 and 2). Parameter Σ determines how many sites belonging to each lattice, 1 and 2, is the share of one CSL site. The minimum possible value $\Sigma = 3$ for the fcc lattice corresponds to a twin boundary (or stacking fault). It turned out that the $\sigma_{GB}(\theta)$ curve in the vicinity of θ_Σ exhibits deep dips [8–10]. Their shape is also described by Read–Shockley relation (1) but with the difference $|\theta - \theta_\Sigma|$ instead of the angle θ and with the Burgers vector $b_\Sigma = b/\Sigma$ of grain boundary dislocations, which is the lattice vector for the displacement shift lattice

reciprocal to CSL [11, 12] instead of the Burgers vector b of lattice dislocations. A similar dependence with the dips also appears when the plane of the tilt grain boundary is rotated about the $\langle hkl \rangle$ axis, whereas the misorientation angle θ remains fixed [13, 14].

Gradually (by default), it was commonly accepted that the energy spectrum of the tilt boundaries beginning from zero energy or from $\sigma_{GB}(\theta_{\Sigma=3})$ to $\sigma_{GB}(\theta_{max})$ is just the energy spectrum of grain boundaries in a polycrystal as a whole (or, at least, its main part). This is because any simple experimental technique for comparing energies of tilt grain boundaries with different misorientation axes and the total energy of tilt boundaries with that of a general type without the coinciding lattice planes was absent until recently. In [1–10, 13, 14], the energy of grain boundaries was measured by the technique of thermal etching groove. This method always gives the relative value expressed in units of the energy of the outer surface, to which the grain boundary comes out in the course of measurements. The other methods (for example, zero-creep measurements [15–18]) allow one to determine the average value of σ_{GB} for polycrystals without giving information on the full amplitude of σ_{GB}.

An experimental method for comparison of energies σ_{GB} for quite different kinds of grain boundaries has been developed recently. It is based on measuring temperatures of the transition from the incomplete to complete wetting of grain boundaries by the liquid phase (melt) [19–22]. If the two- or multicomponent solid solution is in an equilibrium contact with the melt, two situations are possible.

1. The melt partially wets internal interfaces between crystallites (grain boundaries) in the polycrystal. This means that the grain boundary energy σ_{GB} is lower than the energy $2\sigma_{SL}$ of two interfaces between the solid phase and the melt. In this case, the contact angle φ at the place where the grain boundary comes out to the interface between the solid and liquid phases is determined by the relation

$$\sigma_{GB} = 2\sigma_{SL}\cos(\varphi/2). \quad (2)$$

2. The melt completely wets the grain boundaries. Then, $\sigma_{GB} \le 2\sigma_{SL}$ and the contact angle vanishes ($\varphi = 0$). In this case, the melt layer should substitute for the grain boundary, separating the crystallites from each other.

In 1977, it was demonstrated for the first time that the transition from the incomplete to complete wetting is a phase transition, which can occur at variations of the temperature or pressure [23, 24]. It is possible if the $\sigma_{GB}(T)$ and $2\sigma_{SL}(T)$ curves cross at some temperature T_w below the melting temperature T_m. The value of T_w depends on the grain boundary energy: the higher σ_{GB}, the lower T_w. The wetting transition in polycrystals starts at $T_{w,min}$, when the complete wetting occurs at grain boundaries with the maximum energy

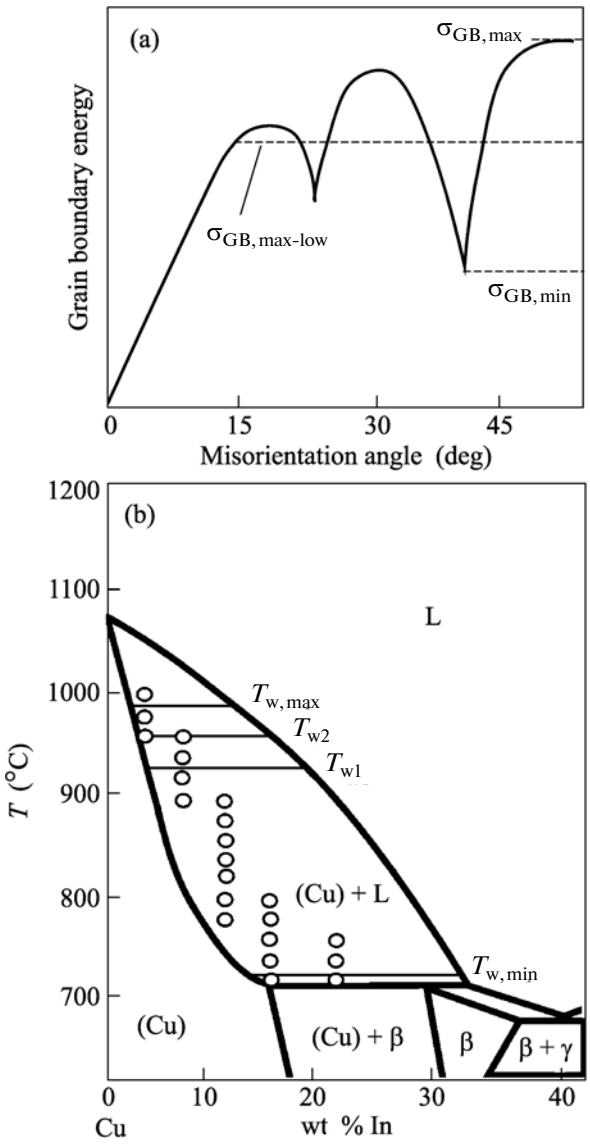

Fig. 1. (a) Schematic curve illustrating the dependence of the grain boundary energy on the misorientation angle. The dips correspond to special types of grain boundaries close to the coincidence misorientations. (b) Part of the phase diagram for Cu–In alloys [26]. Solid lines correspond to the phase transitions in the bulk, thin lines denote tie lines for the wetting transitions at grain boundaries, and points indicate the annealing temperatures and the compositions of the alloys under study.

$\sigma_{GB,max}$. It terminates at $T_{w,max}$, when the complete wetting occurs at grain boundaries with the minimum energy $\sigma_{GB,min}$ (Fig. 1a). The comparison of T_w values measured at specially grown bicrystals [25] with individual tilt boundaries [19–22] having the minimum and maximum energies with $T_{w,min}$ and $T_{w,max}$ measured at polycrystals with a large number of grain boundaries just provides a tool to determine the width of the spectrum of tilt grain boundaries and their con-

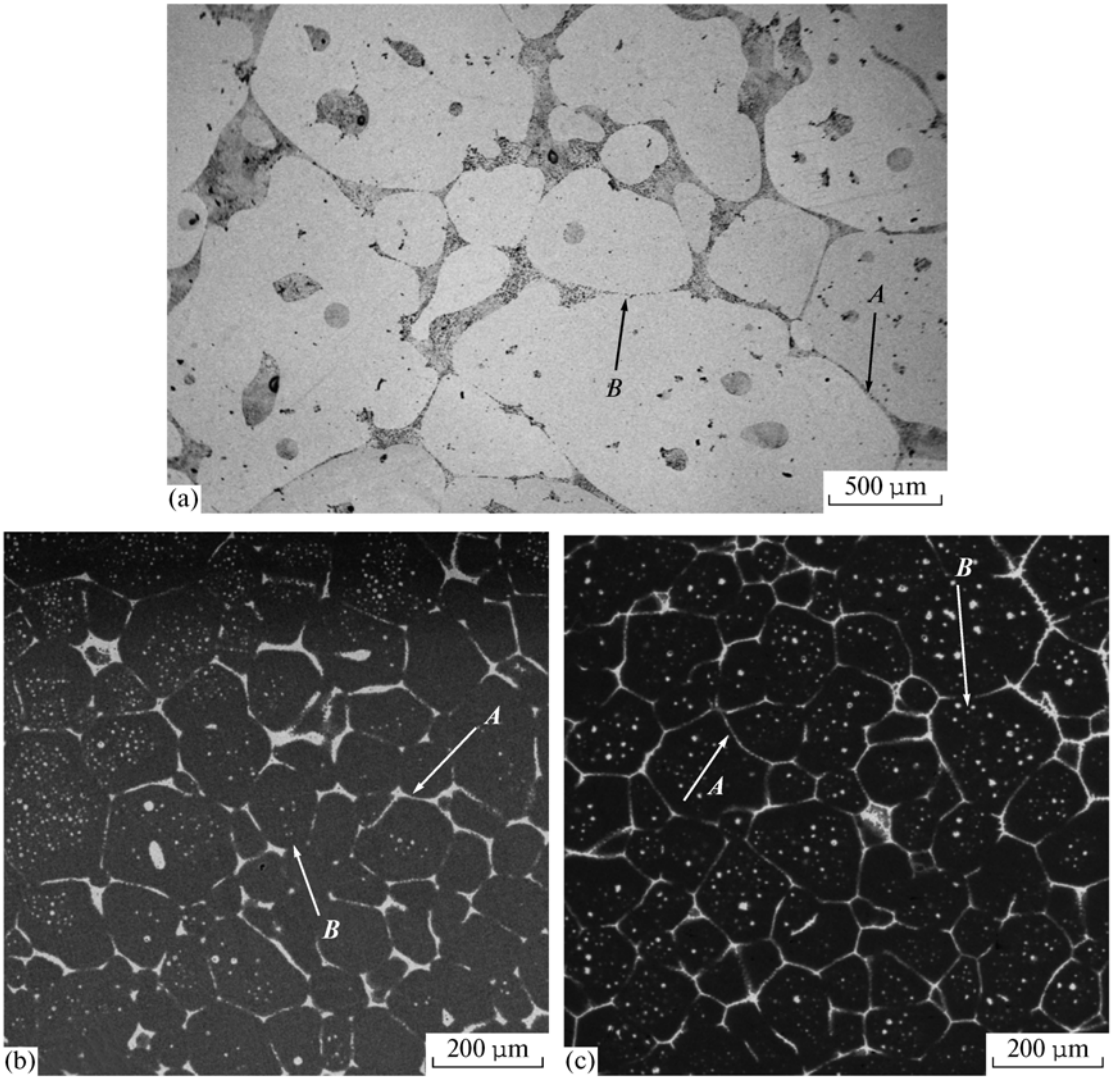

Fig. 2. (a) Microstructure of Cu–2 wt % Zn alloy after annealing at 220°C in the two-phase region of the phase diagram. (b, c) Microstructure of Cu–4 wt % In alloy after annealing in the two-phase region of the phase diagram at 772 and 972°C, respectively. The arrows indicate completely (*A*) and incompletely (*B*) wetted grain boundaries.

tribution to the total energy spectrum of grain boundaries in polycrystals.

For the studies using induction melting in vacuum, we prepared alloys of copper with 4, 8, 12, 16, and 22 wt % of indium. We used copper with a purity of 99.998 wt % and indium with a purity of 99.999 wt %. We also prepared an alloy of tin with 2 wt % of zinc (using both tin and zinc with a purity of 99.999 wt %). The prepared ingots 10 mm in diameter were cut into disks 2 mm thick, which were sealed into evacuated quartz ampoules. The ampoules with the samples were annealed in a SUOL resistance furnace for 2 h at temperatures ranging from 715 to 1000°C (copper–indium alloys) and for 7 h at 201, 207, 212, 215, 217, 222, and 227°C (tin–zinc alloy). The points corresponding to the values of annealing temperature and to the content of copper–indium alloys are shown in Fig. 1b. After annealing, the samples were quenched in water (the ampoules were broken) and then were mechanically ground and polished using a diamond paste with grit down to 1 μm. The obtained slices were studied by optical spectroscopy using a Neophot-32 microscope equipped with a 10 Mpix Canon Digital Rebel XT digital camera, as well as by scanning electron microscopy and by electron probe microanalysis (EPMA) using a Tescan Vega TS51030 MM device equipped with a LINK energy-dispersion spectrometer (Oxford Instruments). A grain boundary on the copper-based (Cu) or tin-based (Sn) solid solution was treated as completely wetted if the melt layer completely covered the boundary from one triple junction to another (boundaries *A* in Fig. 2). The boundary was

considered as partially wetted if the melt layer was terminated (boundaries *B* in Fig. 2).

Figure 2b illustrates the microstructure of Cu–12 wt % In alloy after annealing at 772°C. It includes two structural components, dark and light. The dark structural component (host) is the copper-based solid solution with the indium content corresponding to the solidus line at the annealing temperature (i.e., about 7 wt % of In). The light component, located at grain boundaries and triple junction, was formed in the course of quenching from the indium-rich melt with the composition corresponding to the liquidus line. In the structure shown in Fig. 2b, there are a very small number of grain boundaries completely wetted by the melt. The melt forms isolated although very flat droplets at grain boundaries. The first grain boundaries completely wetted by the melt appear at $T_{w,min}$ = 715°C (see Fig. 1b). For $T_{w,min}$ = 715°C, on the phase diagram presented in Fig. 1b, we show a tie line for the onset of the wetting phase transition for high-angle grain boundaries. At this temperature, the grain boundaries with the highest energy become completely wetted (see the schematic curve in Fig. 1a).

Figure 2c illustrates the microstructure of Cu–4 wt % In alloy after annealing at 972°C. In this structure, nearly all high-angle boundaries are completely wetted. The last large-angle grain boundaries partially wetted by the melt disappear at $T_{w,max}$ = 986°C (see Fig. 1.b). For $T_{w,max}$ = 986°C, on the phase diagram presented in Fig. 1b, we show a tie line for the offset of the wetting phase transition for high-angle grain boundaries. At this temperature, the grain boundaries with the lowest energy become completely wetted (see Fig. 1a). Figure 3a shows the temperature dependence of the percentage of the wetted grain boundaries in Cu. It grows from zero at $T_{w,min}$ = 715°C to 100% at $T_{w,max}$ = 986°C.

The measurements of T_w were reported in [22] for two tilt grain boundaries in copper with the misorientation axis ⟨110⟩ and with the misorientation angles θ = 77° and 141°. These values are T_{w2} = 960°C and T_{w1} = 930°C, respectively. The misorientation angle θ = 77° is close to θ = 70.5° characteristic of the symmetric twin boundaries and the corresponding energy σ_{GB2} is close to the minimum value possible for the tilt grain boundaries in copper. The energy σ_{GB1} for the boundary with θ = 141° is higher by 40%. It is close to the maximum energy possible for the tilt grain boundaries with ⟨110⟩. Both tie lines, at T_{w2} = 960°C and T_{w1} = 930°C, are shown in Fig. 1b. We see that the difference $T_{w2} - T_{w1}$ = 30°C is very small (about 11%) in comparison to the difference $T_{w,max} - T_{w,min}$ = 271°C (see Figs. 1b and 3a). At the same time, both temperatures, T_{w2} = 960°C and T_{w1} = 930°C, are very close to $T_{w,max}$ = 986°C.

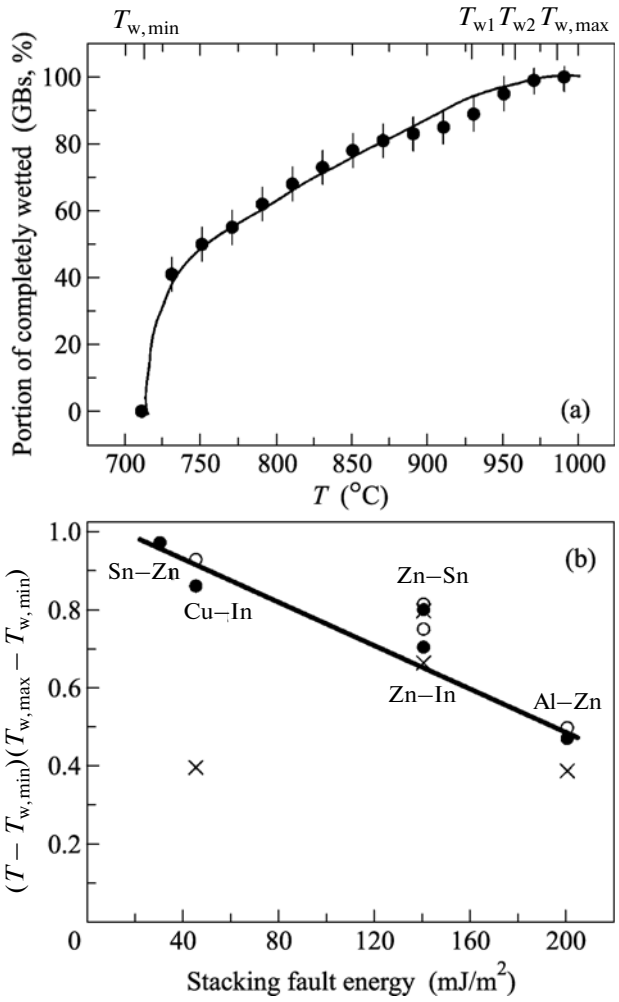

Fig. 3. (a) Temperature dependence of the percentage of the wetted grain boundaries in copper–indium alloys. We show the onset ($T_{w,min}$ = 715°C) and offset ($T_{w,max}$ = 986°C) temperatures of the wetting transition in polycrystals, as well as the wetting transition temperatures at individual tilt grain boundaries with misorientation angles θ = 77° and 141° (T_{w2} = 960°C and T_{w1} = 930°C). (b) (Open circles) Maximum and (closed circles) minimum wetting transition temperatures T_w for the tilt grain boundaries in metals with different stacking fault energies. The values of T_w are normalized to the difference between the maximum ($T_{w,max}$) and minimum ($T_{w,min}$) values of the wetting transition temperature in polycrystals. The crosses indicate the temperatures at which half of the grain boundaries in polycrystals are wetted.

In Sn–2 wt % Zn alloy (see Fig. 2a), the complete wetting of all grain boundaries occurs at $T_{w,max}$ = 220°C. However, even at 201°C (i.e., at a temperature slightly exceeding the eutectic temperature of 198.5°C [26]), 90% of grain boundaries in tin are already wetted by the melt. This means that $T_{w,min}$ is lower than the eutectic temperature. It can be formally determined by the extrapolation to zero of the temperature dependence of the percentage of the wetted grain

boundaries. The measurements of T_w were reported in [27] for two tilt grain boundaries in tin with the misorientation axis $\langle 100 \rangle$ and with the misorientation angles close to those characteristic of the coincidence misorientations $\Sigma 5$ and $\Sigma 17$. The values of T_{w1} and T_{w2} almost coincided and were equal to 217°C. This temperature is also very close to $T_{w,max}$, as in copper–indium alloys.

Figure 3b shows temperatures for the transition from the incomplete to complete wetting as functions of the stacking fault energies. On the vertical axis, zero and unity correspond to $T_{w,min}$ and $T_{w,max}$, respectively. In copper, the stacking fault energy according to different sources ranges from 30 to 45 mJ/m^2 [28], and for tin, we have 30 mJ/m^2 [29]. In addition to the data obtained in the present work for copper–indium and tin–zinc alloys, Fig. 3b also shows the points corresponding to other systems studied by us earlier. In [30], for example, the values $T_{w,min} = 440$°C and $T_{w,max} = 620$°C were reported for Al–Zn polycrystals, and the temperatures $T_{w1} = 530$°C and $T_{w2} = 525$°C were measured in [31] for $\langle 110 \rangle$ tilt boundaries in aluminum corresponding to misorientation angles equal to 15° and 35°. According to the data reported in [8], the energy of tilt grain boundaries at these two misorientation angles is close to the maximum and minimum values, respectively. The stacking fault energy in aluminum is 140 mJ/m^2 [32].

In zinc–indium alloys ($T_{eutct} = 143.5$°C and $T_{melf}(Zn) = 419.58$°C [26]), already 18% of grain boundaries are wetted at 210°C, whereas at 360°C, the percentage of wetted boundaries is 63% [33]. This means that both $T_{w,min}$ and $T_{w,max}$ can be found only by extrapolation (as a result, we have 150 ± 20°C and 550 ± 20°C, respectively). The temperatures of the transition from the incomplete to complete wetting were measured for the $[10\bar{1}0]$ tilt grain boundaries in zinc with the misorientation angles $\theta_1 = 19°$ and $\theta_2 = 66°$ and for the tilt grain boundary [1, 1, –2, 0] with $\theta_3 = 79°$ [33]. Angles θ_2 and θ_3 are close to those corresponding to the coincidence misorientations, whereas θ_1 characterizes a grain boundary of a general type [34]. The transition temperatures are $T_{w1} = 362$°C, $T_{w2} = 376$°C, and $T_{w3} = 375$°C, respectively. The stacking fault energy in zinc according to different sources ranges from 160 to 200 mJ/m^2 [29].

In zinc–tin alloys ($T_{eutct} = 198.5$°C [26]), already 19% of grain boundaries are wetted at 260°C, whereas at 395°C, the percentage of wetted boundaries is 68% [33]. Therefore, both $T_{w,min}$ and $T_{w,max}$ can be found only by extrapolation (as a result, we have 100 ± 20°C and 450 ± 20°C, respectively). The temperatures of the transition from the incomplete to complete wetting were determined for the [1, 0, –1, 0] tilt grain boundaries in zinc with the misorientation angles $\theta_1 = 16°$ and $\theta_2 = 60°$ [19]. Angle θ_2 is close to that corresponding to the coincidence misorientations, whereas θ_1 characterizes a grain boundary of a general type [34]. The transition temperatures are $T_{w1} = 386.5$°C and $T_{w2} = 381$°C, respectively.

To summarize, the width of the spectrum of tilt grain boundaries and their contribution to the total energy spectrum of grain boundaries in polycrystals have been estimated for the first time by measuring temperatures T_w for the transition from the incomplete to complete wetting of grain boundaries in poly- and bicrystals. It turned out that all tilt grain boundaries (from those with coincidence misorientations with the lowest grain boundary energy to the grain boundaries of the general type with the highest energy) correspond to a rather narrow (only 5–10%) portion in the total energy spectrum of grain boundaries in polycrystals. In metals with a low stacking fault energy (copper, tin, zinc), the tilt grain boundaries belong to 10–20% of the grain boundaries with the highest transition temperatures T_w (hence with low energies). In the metal with a high stacking fault energy (aluminum), the values of T_w for the tilt grain boundaries lie nearly in the middle between the minimum ($T_{w,min}$) and maximum ($T_{w,max}$) transition temperatures from the incomplete to complete wetting of grain boundaries. This means that grain boundaries with the structure corresponding to a lower energy than that of the symmetric twin boundaries (or stacking faults) can exist in aluminum.

We are grateful to A.N. Nekrasov for his help in performing experiments and to Profs. B.S. Bokshtein and A.L. Petelin for helpful discussions. This work was supported by the Russian Foundation for Basic Research (project nos. 11-03-01198 and 11-08-90439), by the State Foundation for Basic Research of Ukraine (project no. F407040), and by the National University of Science and Technology MISiS (Development Program).

REFERENCES

1. K. T. Aust and B. Chalmers, Proc. R. Soc. A **201**, 210 (1950); Proc. R. Soc. A **204**, 359 (1950).
2. C. G. Dunn, F. W. Daniels, and M. J. Bolton, J. Metals **2**, 1245 (1950).
3. A. P. Greenough and R. King, J. Inst. Metals **79**, 415 (1951).
4. C. G. Dunn and F. Lionetti, J. Metals **1**, 125 (1949).
5. R. C. Pond and D. A. Smith, Int. Met. Rev. **21**, 61 (1976).
6. J. P. Hirth and J. Lothe, *Theory of Dislocations* (McGraw Hill, New York, 1968; Atomizdat, Moscow, 1972).
7. E. Rabkin and I. Snapiro, Acta Mater. **48**, 4463 (2000).
8. G. Hasson, J.-Y. Boos, and I. Herbeuval, Surf. Sci. **31**, 115 (1972).

9. T. Muschik, W. Laub, U. Wolf, et al., Acta Metall. Mater. **41**, 2163 (1993).
10. A. Barg, E. Rabkin, and W. Gust, Acta Metall. Mater. **43**, 4067 (1995).
11. A. N. Orlov, V. N. Perevezentsev, and V. V. Rybin, *Grain Boundaries in Metals* (Metallurgiya, Moscow, 1980) [in Russian].
12. W. Bollmann, *Crystal Defects and Crystalline Interfaces* (Springer, Berlin, 1970).
13. A. Otsuki and M. Mitsuno, Trans. Jpn. Inst. Met. (Suppl.) **27**, 789 (1986).
14. A. Otsuki, Interface Sci. **9**, 293 (2001).
15. I. Sawai and M. Nishida, J. Anorg. Chem. **190**, 375 (1930).
16. G. Tammann and W. Boehme, Ann. Phys. **12**, 820 (1932).
17. H. Udin, A. J. Shaler, and J. Wulff, J. Metals **1**, 1936 (1949).
18. B. S. Bokshtein, D. V. Vaganov, and S. N. Zhevnenko, Phys. Met. Metallogr. **104**, 564 (2007).
19. B. B. Straumal, W. Gust, and T. Watanabe, Mater. Sci. Forum **294**, 411 (1999).
20. B. B. Straumal, W. Gust, and D. A. Molodov, Interf. Sci. **9**, 127 (1995).
21. B. Straumal and W. Gust, Mater. Sci. Forum **207**, 59 (1996).
22. B. Straumal, T. Muschik, W. Gust, et al., Acta Metall. Mater. **40**, 939 (1992).
23. J. W. Cahn, J. Chem. Phys. **66**, 3667 (1977).
24. C. Ebner and W. F. Saam, Phys. Rev. Lett. **38**, 1486 (1977).
25. V. N. Semenov, B. B. Straumal, V. G. Glebovsky, et al., J. Cryst. Growth **151**, 180 (1995).
26. *Binary Alloy Phase Diagrams*, Ed. by B. Massalski et al. (ASM International, Materials Park, 1993).
27. V. A. Murashov, B. B. Straumal, and P. V. Protsenko, Bull. Russ. Ac. Sci.: Phys. **74**, 1551 (2010).
28. C. B. Carter and I. L. F. Ray, Philos. Mag. **35**, 189 (1977).
29. L. E. Murr, *Interfacial Phenomena in Metals and Alloys* (Addison-Wesley, Boston, 1975).
30. B. Straumal, G. Lopez, W. Gust, et al., in *Nanomaterials by Severe Plastic Deformation. Fundamentals—Processing—Applications*, Ed. by M. J. Zehetbauer and R. Z. Valiev (Wiley-VCH, Weinheim, 2004), p. 642.
31. B. B. Straumal, A. S. Gornakova, O. A. Kogtenkova, et al., Phys. Rev. B **78**, 054202 (2008).
32. J. Cai, F. Wang, C. Lu, et al., Phys. Rev. B **69**, 224104 (2004).
33. A. S. Gornakova, B. B. Straumal, S. Tsurekawa, et al., Rev. Adv. Mater. Sci. **21**, 18 (2009).
34. G. Gottstein and L. Shvindlerman, *Grain Boundary Migration in Metals: Thermodynamics, Kinetics, Applications* (Oxford Univ. Press, Oxford, 2011).

Translated by K. Kugel